Spectroscopic and Electrochemical Properties of Dimeric Ruthenium(II) Diimine Complexes and Determination of Their Excited State Redox Properties

Yael Fuchs, Sonita Lofters, Thomas Dieter, Wei Shi, Robert Morgan, Thomas C. Strekas,* Harry D. Gafney,* and A. David Baker*

Contribution from the Department of Chemistry, City University of New York, Queens College, Flushing, New York 11367. Received June 9, 1986

Abstract: The complexes $Ru(bpy)_2(ppz)^{2+}$ and $[(bpy)_2Ru(ppz)Ru(bpy)_2]^{4+}$, where ppz is the planar ligand 4′,7′-phenanthrolino-5′,6′:5,6-pyrazine, have been prepared and characterized. Resonance Raman spectra establish that the visible spectra of $Ru(bpy)_2L^{2+}$ and $[(bpy)_2Ru-L-Ru(bpy)_2]^{4+}$ complexes, where L is a bis-diimine, in general, are composed of MLCT transitions which terminate in the π^* orbitals localized on the different ligands. The luminescence, which is detectable at room temperature in fluid solutions of both the mono- and bimetallic complexes, can be assigned as a $L(\pi^*) \rightarrow Ru(II)$ t_2 transition. An approximate but general correlation between the lower energy MLCT absorption maximum and the emission maximum suggests that in many other bimetallic complexes of Ru(II) the emission energy is shifted beyond usual detection limits. Analysis of the emission and electrochemical data indicates that the MLCT states of bridged 2,3-dipyridylpyrazine (dpp) and ppz dimeric complexes are weak reductants but very strong oxidants. The implications of this general pattern of excited state redox potentials are discussed.

The luminescence from diimine complexes of Ru(II) has provided a unique probe of this transition metal's excited states.[1-3] Quantum yield and emission decay measurements provide access to the dynamics of intramolecular energy migration and dissipation. Quenching of the luminescent MLCT state offers, depending on the characteristics of the quencher, insights into the dynamics of intermolecular energy and electron transfer. Depending on the excited state potential (i.e., the difference in energy between the emissive state and the ground state oxidized and/or reduced states of the complex) as compared to that of the quencher, electron transfer may occur at a rate which may be predicted according to Marcus theory. However, electron transfer quenching studies of ruthenium(II) diimines provide evidence[1-3] of only one photon–one electron events. Since many important redox reactions involve multielectron transfer,[4,5] there is an interest in homogeneous and heterogeneous systems which convert multiple, photoinduced, single electron transfer events into subsequent multielectron transfer reactions. One such avenue of investigation involves polymeric Ru(II) complexes[6-14] which may be capable of acting as multielectron donors. Regardless of the kinetic constraints, which may be severe, the excited state redox potentials of such compounds are of pivotal significance in determining the photoinduced redox chemistry which may be available.

Monomeric ruthenium(II) diimine complexes exhibit intense MLCT transitions in the 400–600-nm region and corresponding emissions in the 600–700-nm region. Formation of the corresponding polymeric complexes results in the red shift of the lowest energy MLCT absorption band and the observation of a single red shifted emission. In each case, the red shift is associated with transitions involving the lowest energy π^* orbital of the bridging ligand. Although a number of bimetallic ruthenium(II) diimine complexes have been reported,[6-11] only one[6] has been found to be emissive in fluid solution at room temperature. Consequently, the excited state potentials of most bimetallic ruthenium(II) diimines, which determine their photoinduced redox chemistry, are not known.

Since subtle changes in coordination about Ru(II) can lead to a loss of luminescence, our strategy has focused on the design of bridging ligands which closely mimic the coordination of 2,2′-bipyridine at each Ru(II) center. To this end, the bridging ligand 2,3-di-2-pyridylpyrazine (dpp) was synthesized[6] and used to prepare $Ru(bpy)_2(dpp)^{2+}$ and $[(bpy)_2Ru(dpp)Ru(bpy)_2]^{4+}$. In

(1) Kalyanasundaram, K. *Coord. Chem. Rev.* **1982**, *46*, 159.
(2) Sutin, N.; Creutz, C. *Pure Appl. Chem.* **1980**, *52*, 2717.
(3) Watts, R. J. *J. Chem. Educ.* **1983**, *60*, 834.
(4) Meyer, T. J. *J. Electrochem. Soc.* **1984**, 221C.
(5) Ibers, J. A.; Holm, R. H. *Science* **1980**, *209*, 233.
(6) Braunstein, C. H.; Baker, A. D.; Strekas, T. C.; Gafney, H. D. *Inorg. Chem.* **1984**, *23*, 857.
(7) Rillema, D. P.; Mack, K. B. *Inorg. Chem.* **1982**, *21*, 3849.
(8) Rillema, D. P.; Callahan, R. W.; Mack, K. B. *Inorg. Chem.* **1982**, *21*, 2589.
(9) Dose, E.; Wilson, L. J. *Inorg. Chem.* **1978**, *17*, 2660.
(10) Hunziger, M.; Ludi, A. *J. Am. Chem. Soc.* **1977**, *99*, 7370.

(11) Haga, M.-A. *Inorg. Chim. Acta* **1980**, *45*, L183.
(12) Tinnemans, A. H. A.; Timmer, K.; Reinten, M.; Kraaijkamp, J. G.; Alberts, A. H.; van der Linden, J. G. M.; Schmitz, J. E. J.; Saaman, A. A. *Inorg. Chem.* **1981**, *20*, 3698.
(13) Curtis, J. C.; Bernstein, J. S.; Meyer, T. J. *Inorg. Chem.* **1985**, *24*, 385.
(14) Petersen, J. D.; Murphy, W. R., Jr.; Brewer, K. J.; Ruminski, K. R. *Coord. Chem. Rev.* **1985**, *64*, 261.

2692   *J. Am. Chem. Soc., Vol. 109, No. 9, 1987*

Fuchs et al.

contrast to complexes with the structurally similar ligand, 2,3-di-2-pyridylquinoxaline,[7,8] both of these complexes are luminescent in fluid solution at room temperature.

A comparison of the spectral and electrochemical properties of $Ru(bpy)_2(L)^{2+}$ and $[(bpy)_2Ru-L-Ru(bpy)_2]^{4+}$ complexes for which L is one of several bis-diimine ligands (Table III), establishes that the perturbation of the π^* acceptor orbital energy which is introduced upon coordination of the second $Ru(bpy)_2^{2+}$ moiety depends on the nature of the bridging ligand. For example, when L = 2,2'-bipyrimidine (bpym) or 4,4'-dimethyl-2,2'-bipyrimidine (dmbpym) the π^* orbital of these ligands is lowered 8290 and 6780 cm^{-1} upon addition of the second Ru(II) center. This contrasts sharply with the more modest drop of some 2230 cm^{-1} for the π^* orbital of dpp, which is comparable to the kind of energy change observed[1] when a moderate electron withdrawing substituent is substituted at the periphery of 2,2'-bipyridine in a tris complex of Ru(II). When the strongly electron withdrawing NO_2 is substituted[15,16] at the 4 position of bpy, the π^* orbital is lowered by 3760 cm^{-1} and the tris complex of Ru(II) is nonluminescent in fluid solution at room temperature. The resonance Raman spectra of this complex indicate[17] that a significant portion of the charge is localized on the nitro group in the absorptive excited state. Since NO_2 groups are strongly coupled to solvent, efficient radiationless deactivation occurs. In a bimetallic complex with two strongly coupled metal centers, as indicated by a large drop in the bridging ligand π^* acceptor orbital energy, the second metal center may act in a similar manner, i.e., offer an efficient pathway for radiationless deactivation. With the bridging ligand dpp (and as reported here, ppz) this is not the case, and emission is observed.

Steric constraints arising from the bridging ligand in $[(bpy)_2Ru(dpp)Ru(bpy)_2]^{4+}$ had been considered[6] as a possible factor leading to the relatively small perturbation of the π^* orbital. To probe the role of an assumed tortional twist in the dpp bridge in moderating interaction between the metal centers, and to gain further insight into the excited state energies and redox potentials of binuclear complexes of Ru(II), the planar bridging ligand 4',7'-phenanthrolino-5',6':5,6-pyrazine (ppz) has been synthesized and monomeric and dimeric complexes prepared. Both are luminescent in fluid solution at room temperature. This result indicates that steric constraints may be of minor importance but that the detailed nature of the electronic structure of the bridging ligand is important in determining the luminescence of such complexes. An approximate correlation between the lowest energy MLCT absorption and the emission energy of such complexes suggests that the existence of a low-energy π^* orbital on the bridging ligand would red-shift the emission energy of many dimers previously reported beyond the usual detection limits. General conclusions regarding the structural, photophysical, and excited state redox properties of binuclear ruthenium(II) diimine complexes are discussed.

Experimental Section

Materials. 4',7'-Phenanthrolino-5,6:5',6'-pyrazine (I) was prepared by a procedure similar to that of Schmidt and Druey.[18] A 10-g (0.05 mol) sample of 4,5-phenanthroline-5,6-dione (Ciba Geigy) was added to 500 mL of methanol containing 3.3 mL (0.05 mol) of ethylenediamine (Aldrich). The reaction was stirred at room temperature, 22 °C, for 2 h, and after evaporation of solvent, a mixture of red and yellow-brown crystals was obtained. The red crystals (a nonaromatic analogue of I) were removed by dissolution in cold acetone. The residue of yellow-brown crystals, after recrystallization from acetone, yielded almost colorless needles, mp 268 °C. The ^1H NMR spectrum of I is consistent with that expected, showing only aromatic resonances.

Formation of the monometallic complex was attempted by refluxing 1 equiv of ligand I with 1 equiv of *cis*-Ru(bpy)$_2$Cl$_2$. However, spectra recorded after refluxing for 72 h in 95% ethanol indicated that the major reaction product was $[(bpy)_2Ru(ppz)Ru(bpy)_2]^{4+}$. Consequently, the monometallic complex was prepared in the above manner with a 2:1 ratio of ppz to ruthenium. UV–vis spectra recorded periodically during the
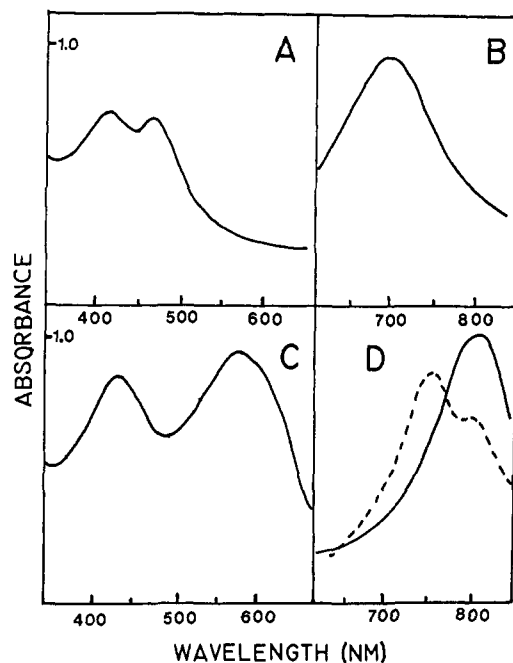

Figure 1. Absorption (A) and solution emission (B) spectra of Ru-$(bpy)_2(ppz)^{2+}$ and absorption (C) and emission (D, solid line) spectra of $(bpy)_2Ru(ppz)Ru(bpy)_2^{4+}$. The broken line is 77 K emission spectrum in 1:1 glycerol:water.

reflux indicated that the maximum amount of $Ru(bpy)_2(ppz)^{2+}$ was formed in 48 h. At this point, the reaction mixture was filtered, and the monometallic complex was precipitated by addition of an aqueous solution of sodium perchlorate (caution should be observed when handling perchlorate salts of this type!). After recrystallization from 1:1 water: methanol, the red complex $[Ru(bpy)_2(ppz)^{2+}](ClO_4)_2$ was obtained in 84% yield.

The bimetallic complex, $[(bpy)_2Ru(ppz)Ru(bpy)_2](ClO_4)_4$ was prepared in a similar manner, except that 2 equiv of $Ru(bpy)_2Cl_2$ were refluxed with 1 equiv of ppz in 95% ethanol for 72 h. The reaction mixture was filtered and, after being cooled to room temperature, the blue, bimetallic complex was precipitated by addition of aqueous sodium perchlorate. This was purified further by repeated recrystallizations from 1:1 ethanol–water mixtures. The purity of recrystallized sample was then confirmed by a previously described[19] chromatographic procedure. The dpp complexes were prepared as described previously.[6]

Physical Measurements. Absorption spectra were recorded on a Cary 14 or a Perkin-Elmer Lambda 3 UV–vis spectrophotometer. Room temperature and low-temperature (77 K) emission spectra were recorded on a previously described[19] Perkin-Elmer Hitachi MPF-2A emission spectrophotometer. Emission quantum yields were measured relative to $[Os(bpy)_3](ClO_4)_2$ according to the procedure of Demas and Crosby.[20] Luminescent lifetimes were measured with previously described equipment.[19]

The resonance Raman spectrophotometer has been previously described.[21] Spectra were obtained with 90° transverse excitation with samples in 1 mm i.d. capillary tubes.

Cyclic voltammetry measurements were made with previously described[6] PAR equipment. Millimolar solutions of the Ru(II) complexes (as perchlorate salts) were prepared in 0.1 M acetonitrile solutions of tetra-*n*-butylammonium tetrafluoroborate. The acetonitrile was freshly distilled over P_2O_5, and the solutions were deaerated by purging with nitrogen. All voltammograms were recorded under a nitrogen atmosphere with a Pt microcylinder working electrode, a Pt wire auxiliary electrode, and a standard calomel reference electrode.

Results

Absorption and Emission Spectra. Visible absorption spectra of $Ru(bpy)_2(ppz)^{2+}$ and $[(bpy)_2Ru(ppz)Ru(bpy)_2]^{4+}$ (Figure 1) are similar to those of previously characterized mono- and bi-

(15) Weiner, M. A.; Basu, A. *Inorg. Chem.* **1980**, *19*, 2797.
(16) Basu, A.; Weiner, M. A.; Strekas, T. C.; Gafney, H. D. *Inorg. Chem.* **1982**, *21*, 1085.
(17) Basu, A.; Gafney, H. D.; Strekas, T. C. *Inorg. Chem.* **1982**, *21*, 1085.
(18) Schmidt, P.; Druey, J. *Helv. Chim. Acta* **1957**, *40*, 350.

(19) Wolfgang, S.; Strekas, T. C.; Gafney, H. D.; Krause, R.; Krause, K. *Inorg. Chem.* **1984**, *23*, 2650.
(20) Demas, J. N.; Crosby, G. A. *J. Am. Chem. Soc.* **1971**, *93*, 2841.
(21) Valance, W. G.; Strekas, T. C. *J. Phys. Chem.* **1982**, *86*, 1804.
(22) Knors, C.; Gafney, H. D.; Baker, A. D.; Braunstein, C. H.; Strekas, T. C. *J. Raman Spectrosc.* **1983**, *14*, 32.

Table I. Relative Quantum Yields of Dimer Emission[a]

	Q_{em}[b]
$(bpy)_2Ru(dpp)Ru(bpy)_2^{4+}$	0.0070 ± 0.0008
$(bpy)_2Ru(ppz)Ru(bpy)_2^{4+}$	0.0157 ± 0.0012

[a] Room temperature, air saturated solution in water. [b] Excitation wavelength was 457.9 nm. For dpp dimer, emission monitored at 755 nm and for ppz dimer at 820 nm.

metallic Ru(II) mixed ligand complexes. The monometallic complex exhibits overlapping absorptions with a maximum at 420 nm ($\epsilon = 1.1 \times 10^4$ M^{-1} cm^{-1}) and a shoulder at 474 nm, which become well-resolved bands in the bimetallic complex with maxima at 418 nm ($\epsilon = 1.3 \times 10^4$ M^{-1} cm^{-1}) and 573 nm ($\epsilon = 1.6 \times 10^4$ M^{-1} cm^{-1}).

The emission spectrum of a deaerated aqueous solution of $Ru(bpy)_2(ppz)^{2+}$ (Figure 1) consists of a single band with a maximum at 700 nm. The excitation spectrum of this emission shows that excitation of either the 420- or 474-nm bands leads to population of the same luminescent state. The emission spectrum of $[(bpy)_2Ru(ppz)Ru(bpy)_2]^{4+}$ at room temperature in aqueous solution also consists of a single band with an apparent maximum at 820 nm. However, the emission occurs in the spectral region where the sensitivity of the photomultiplier tube (RCA C31034) declines rapidly with increasing wavelength. Consequently, the spectrum is skewed to shorter wavelength, and the true emission maximum may lie to longer wavelengths. The emission excitation spectrum parallels the visible absorption spectrum, and the emission quantum yields (Table I) establish that excitation of either visible transition populates the emissive state with equal efficiency. In spite of the lower energy emission, the relative emission quantum yields listed in Table I show that $[(bpy)_2Ru(ppz)Ru(bpy)_2]^{4+}$ is a more efficient emitter than the analogous dpp complex. In addition, freezing a solution of the bimetallic complex to 77 K results in the observation of a resolved vibrational progression (1200 cm^{-1}) (see Figure 1).

The emission of $Ru(bpy)_2(ppz)^{2+}$ decays via first-order kinetics in deaerated aqueous solution at room temperature. Plots of the emission decay, following 337-nm excitation with an Ortec spark gap, yield an emission decay rate constant, k_{em} of $5.0 \pm 1.0 \times 10^6$ s^{-1} and a corresponding lifetime of 200 ± 40 ns. Although the data suggest that the lifetime of $[(bpy)_2Ru(ppz)Ru(bpy)_2]^{4+}$ is ≤ 50 ns under identical conditions, the low energy and intensity of the emission preclude a reliable measurement of its emission decay rate.

Resonance Raman Spectra. Resonance Raman spectra of $Ru(bpy)_2(ppz)^{2+}$ (not shown) and $[(bpy)_2Ru(ppz)Ru(bpy)_2]^{4+}$ (Figure 2) with selected excitation wavelengths show a pattern similar to that previously observed for the mono- and bimetallic dpp complexes. As the excitation wavelength is varied, the resonance Raman vibrational spectrum of the ligand in which the MLCT transition terminates is selectively enhanced. The greater the splitting is between the absorption bands the more well resolved are the Raman spectra of the individual ligands enhanced as a function of excitation wavelength.

Excitation of $Ru(bpy)_2(ppz)^{2+}$ with the 488.0 nm argon ion laser line (to the long wavelength side of the absorption shoulder) enhances vibrations assignable to the ppz at 1532, 1482, 1257, and 1194 cm^{-1}. With 457.9-nm excitation, the bpy vibration at 1491 cm^{-1} is clearly enhanced relative to the 1532-cm^{-1} ppz vibration. Since 457.9 nm is still within the 474 nm absorption band envelope, ppz bands still dominate this spectrum.

For $[(bpy)_2Ru(ppz)Ru(bpy)_2]^{4+}$, dye laser excitation at 562 nm (Figure 2, top) enhances ppz bands, with the most prominent at 1619, 1582, 1480, 1457, 1252, 1220, and 1196 cm^{-1}. With 488.0-nm excitation (Figure 2, middle), which is approximately midway between the MLCT absorptions, bpy vibrations at 1563, 1492, 1317, and 1175 cm^{-1} are evident in the resonance-enhanced spectrum. With 457.9-nm excitation (Figure 2, bottom), the bpy vibrations are approximately equal in intensity to the ppz bands. The above data once again allow the unambiguous assignment of the visible absorptions. In each case, the long wavelength transition is assigned as a metal to ppz MLCT transition.
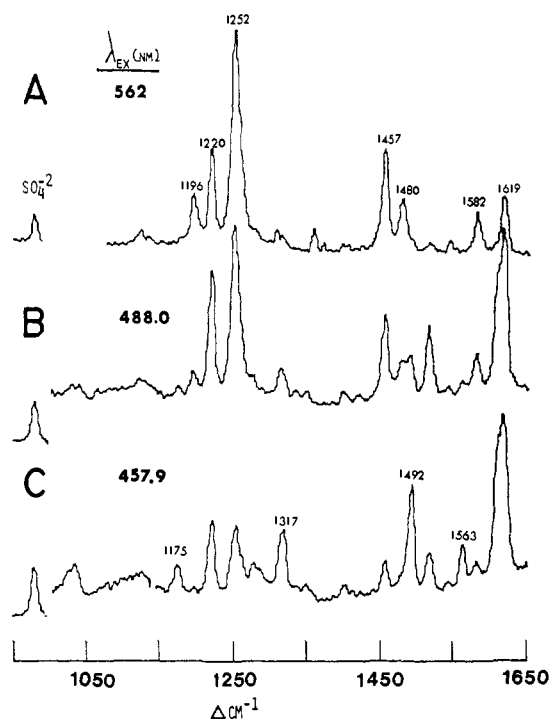
Figure 2. Resonance Raman spectra of $(bpy)_2Ru(ppz)Ru(bpy)_2^{4+}$ with (A) 562 nm, (B) 488.0 nm, and (C) 457.9 nm excitation wavelengths. Complex is 10^{-4} M with 0.5 M sodium sulfate as an intensity reference. Spectral slit width 5 cm^{-1}.

Table II. Cyclic Voltammetry Data for Monomeric and Dimeric Complexes in CH_3CN[a]

complex	oxidations[b] $E_{1/2}$ (V)	reductions $E_{1/2}$ (V)
$(bpy)_2Ru(dpp)^{2+}$	1.34	-1.14, -1.53, -1.74
$(bpy)_2Ru(dpp)Ru(bpy)_2^{4+}$	1.33, 1.52	-0.71, -1.18, -1.55
$(bpy)_2Ru(ppz)^{2+}$	1.37	-1.11, -1.67
$(bpy)_2Ru(ppz)Ru(bpy)_2^{4+}$	1.35, 1.55	-0.67, -1.34, -1.57

[a] All potentials for 10^{-3} M perchlorate salts with 0.1 M tetra-*n*-butylammonium tetrafluoroborate as supporting electrolyte. Volts vs. SCE. [b] Mean of cathodic and anodic half-wave potential values.

Electrochemical Measurements. Cyclic voltammograms of $Ru(bpy)_2(ppz)^{2+}$ and $[(bpy)_2Ru(ppz)Ru(bpy)_2]^{4+}$ closely resemble those of the analogous dpp complexes. The mean half-wave potentials for the oxidations and reductions of the complexes are summarized in Table II. $Ru(bpy)_2(ppz)^{2+}$ exhibits single oxidation and reduction waves separated by 100 mV. Plots of log $[i/(i' - i)]$ vs. V, where i and i' are the current at an applied V and the diffusion-limited current, yield slopes of 0.067 and 0.043 for the anodic and cathodic sweeps, respectively. The values are similar to those we obtained for $Ru(bpy)_3(ClO_4)_2$, 0.063 ± 0.007 and 0.044 ± 0.014, respectively, and along with the ratio of the peak currents, ≥ 0.96, they are criteria which establish the existence of one-electron redox steps.

Under identical conditions, cyclic voltammograms of $[(bpy)_2Ru(ppz)Ru(bpy)_2]^{4+}$ exhibit two overlapping anodic and cathodic waves. Neither wave can be assigned to the oxidation of the ppz ligand since, under these conditions, oxidation of the free ligand occurs at greater than 2.0 V. For those waves that can be resolved, i.e., the first anodic and second cathodic waves, plots of log $[i/(i' - i)]$ vs. V yield slopes of 0.076 and 0.043, respectively. The values are within experimental error of those for $Ru(bpy)_3^{2+}$, and along with the peak currents, >0.95, they indicate reversible, sequential one-electron redox steps for the binuclear complex.

The reduction voltammograms of the mono- and bimetallic dpp and ppz complexes (Figure 3) measured under the same conditions
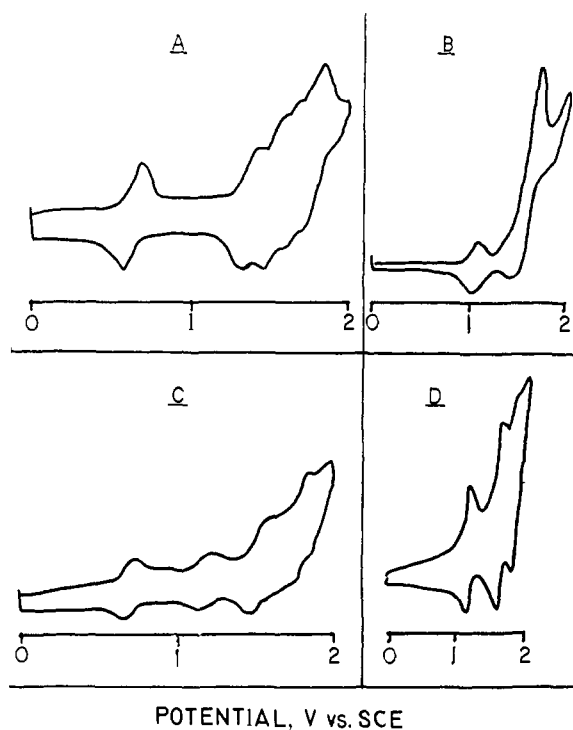
POTENTIAL, V vs. SCE

Figure 3. Reductive cyclic voltammograms for (A) $(bpy)_2Ru(ppz)Ru$-$(bpy)_2^{4+}$, (B) $(bpy)_2Ru(ppz)^{2+}$, (C) $(bpy)_2Ru(dpp)Ru(bpy)_2^{4+}$, and (D) $(bpy)_2Ru(dpp)^{2+}$, all in acetonitrile with Pt anode. Concentration 5 × 10^{-4} M. All potentials vs SCE.

exhibit two or three overlapping waves. Although the reduction voltammograms are more complex, there is no evidence of multielectron events. For each complex, plots of log $[i/(i' - i)]$ vs. V for the resolved portions of the waves, i.e., the first cathodic and last anodic waves, yield slopes which fall within the range expected for one-electron redox processes. The ratio of the peak currents for each complex, ≥ 0.90, indicates that each reduction step is reversible. The average of the cathodic and anodic maxima for these redox steps are listed in Table II.

Discussion

The visible spectra of $Ru(bpy)_2(ppz)^{2+}$ and $[(bpy)_2Ru(ppz)$-$Ru(bpy)_2]^{4+}$ are similar to those of a variety of $Ru(bpy)_2L^{2+}$ and $[(bpy)_2Ru-L-Ru(bpy)_2]^{4+}$ complexes (L = bis diimine) prepared in this and other laboratories. The pattern of band maxima is readily apparent as listed in Table III, which has been included to aid the discussion by comparing relevant properties of all ruthenium(II) complexes of this type reported to date. Each monometallic complex exhibits two MLCT absorptions in the 410–570-nm region, a 6846 cm^{-1} spread, appearing as distinct bands or a major band with a clear shoulder. The higher energy transitions occur within the relatively narrow 415–448-nm range (1775-cm^{-1} spread) and are essentially independent of L. The lower energy transitions exhibit a much wider variation in energy. The transition energy declines as the extent of π delocalization and/or the electron withdrawing character of L increases. Coordination of the second $Ru(bpy)_2^{2+}$ moiety has little effect on the higher energy transition. In fact, this band shifts by no more than 1648 cm^{-1} for a given mono-/bimetallic pair (dmbpyrm complexes). In contrast, the lower energy transitions show pronounced red shifts, as much as 6918 cm^{-1} (bpyrm complexes) on coordination of the second $Ru(bpy)_2^{2+}$. These observations are consistent with d→π^* MLCT transitions in which the higher energy transition terminates in a π^* orbital localized principally on the bpy ligand, whereas the lower energy transition terminates in a π^* orbital principally localized on L. The red shifts observed for the latter transitions reflect the electron withdrawing effect of the second $Ru(bpy)_2^{2+}$ as moderated by the bridging ligand.

The 2,2′-bipyrimidine (bpym) and 2,2′-biimidazole (biim) complexes appear to be exceptions to this general pattern in that a single absorption band is reported for each monometallic com-
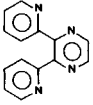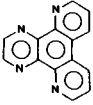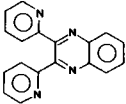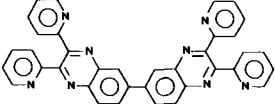
plex. In general, mixed diimine complexes of Ru(II) exhibit multiple visible absorptions, where the separation between the bands reflects the difference between the π systems of the ligands. Since the single bands exhibited by the bpym and biim mixed ligand complexes are broad, we suspect that there are two unresolved underlying absorptions of the MLCT type terminating in the two ligands.
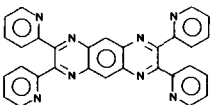
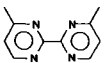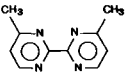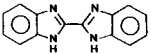Resonance Raman spectra of the mono- and bimetallic complexes of dpp and ppz exhibit a revealing dependence on excitation wavelength. As the excitation wavelength approaches the higher energy transitions, the seven band pattern characteristic of bpy coordinated to Ru(II) becomes more evident in the spectrum. With excitation wavelengths approaching or below the lower energy transition, the relative intensities of the bpy vibrations decline and the relative intensities of the new bands increase. New vibrations appear at 1257, 1482, and 1532 cm^{-1} in the spectrum of $Ru(bpy)_2(ppz)^{2+}$, and at 1266, 1473, and 1519 cm^{-1} in the spectrum of $Ru(bpy)_2(dpp)^{2+}$. Since these bands occur within the region of diimine stretching vibrations, and are not present in the resonance enhanced spectrum of $Ru(bpy)_3^{2+}$, they are assigned to characteristic vibrations of the ppz and dpp ligands. This same pattern is evident in the Raman spectra of the bimetallic complexes, but it is more explicit because the MLCT transitions in resonance are better resolved. The wavelength dependence of the diimine vibrational pattern confirms the assignment of the higher energy MLCT transition to one in which the terminal π^* orbital is on the bpy and the lower energy transition to a MLCT transition in which the π^* orbital lies on the ppz or dpp ligand. Since the majority of complexes in Table III follow the same absorption spectral pattern, the assignments of the MLCT transitions would also.

Coordination of $Ru(bpy)_2^{2+}$ onto $Ru(bpy)_2(ppz)^{2+}$ decreases the MLCT transition energy by 3600 cm^{-1}. Although the limited sensitivity of the photomultiplier tube prevents an exact determination of the emission maximum of the binuclear complex, the decrease is approximately 2000 cm^{-1}. Since these energy changes are similar to and parallel the changes in absorption and emission energies of the dpp analogues, the emissions from the ppz complexes are assigned to the $\pi^*{\to}t_2$ transitions where the π^* orbital is localized on the ppz ligand. As was found for the dpp dimer complexes, the relative emission quantum yields indicate that internal conversion to the ppz localized emissive state from either MLCT state populated upon absorption occurs with equal efficiency. We feel that this internal conversion process may be linked to diimine vibrations which are found to be in resonance with both MLCT absorptions. We have observed that residual intensity of bpy vibrations in resonance Raman spectra obtained with excitation near the maximum of the MLCT transition associated primarily with the bridging ligand is greater than would be predicted on the basis of the excitation wavelength separation from the MLCT to bpy absorption maximum.

We were surprised to find that the ppz complexes are more emissive than the dpp analogues. This was not anticipated since their lower energy emissions were expected to correlate with enhanced nonradiative decay rates. Further emission decay data are necessary to establish the reason, but the data we have suggest that the difference cannot be attributed solely to a difference in the radiative decay rate. The luminescence decay rates of Ru-$(bpy)_2(ppz)^{2+}$ and $[(bpy)_2Ru(ppz)Ru(bpy)_2]^{4+}$, 5.0 ± 1.0 × 10^6 and $\geq 2 \times 10^7$ s^{-1}, respectively, are similar to those of the corresponding dpp complexes, 7.41 ± 0.70 × 10^6 and 1.89 ± 0.36 × 10^7 s^{-1}, respectively. Rather, the difference must lie in the nonradiative dissipation of the excitation energy. In the past, particularly with ruthenium(II) diimine complexes, variations in the radiative rates have been attributed to differences in the hydrophobicity of the ligands. The difference in the nonradiative rates may also reflect the flexibility of the ligand whose π^* acceptor orbital is occupied.[23] Although this flexibility may be difficult to quantitate, previous data suggest that it may be important. For example, phenanthroline is not only more hydrophobic but more

(23) Elfring, W. H.; Crosby, G. A. *J. Am. Chem. Soc.* **1981,** *103,* 2683.

Table III. Spectroscopic and Redox Properties of [Ru(bpy)₂]ₙBLᵐ⁺ Monomers (n = 1, m = 2) and Dimers (n = 2, m = 4)

bridging ligand (BL)^a			MLCT-bpy^b (nm)	MLCT-BL^b (nm)	emission^c max (nm)	$E(3+/2+)^d$ (V)	$E(2+/1+)^d$ (V)	$\Delta\pi^*(BL)^e$ (cm⁻¹)	$E(2+^*/3+)^d$ (V)	$E(2+^*/1+)^d$ (V)
	dpp^f	M^a	430	470	675	1.31	−1.07		0.53	0.76
		D^a	425	525	755	1.30 1.49	−0.64	2230	0.34	1.00
	ppz^f	M	420	474	700	1.34	−1.04		0.43	0.73
		D	418	573	820	1.32 1.52	−0.60	3650	0.19	0.91
	BL(1)^g	M	427	515	(714)	1.38	−0.71		0.36	1.02
		D	423	605	(840)	1.44 1.59	−0.30	3370	0.04	1.17
	BL(3)^h	M	420	525	770	1.38	−0.65		0.23	0.96
		D	424	616	(855)	1.43 1.60	−0.24	3220	0.02	1.21
	BL(2)^g	M	415	573	(795)	1.38	−0.35		0.18	1.21
		D	420	642	(895)	1.42	−0.09	2360	−0.04	1.30
	bpyrm^g,i,j	M	420	420	600	1.33	−0.94		0.74	1.13
		D	408	592	soln (no) solid 769, 870	1.50 1.66	−0.34	8290	0.11	1.27
	dmbpyrm^i	M	442	442	598	1.22	n.r.		0.85	
		D	412	578	(800)	1.40 1.57	n.r.	6780	0.15	
	bbi^k	M	430	460	(641)	1.08	n.r.		0.85	
		D	n.r.	n.r.	n.r.	0.71 1.01	n.r.			
	biim^i	M	448	448	595	0.90	n.r.		0.85	
		D								

no report of dimer

---

^a References as indicated for each entry, M = monomeric (mononuclear) complex; D = dimeric (binuclear) complex. ^b Metal-to-ligand charge transfer absorption maximum. Terminal ligand specified (see text). ^c Emission maximum. Values in parentheses () are estimated from Figure 4 (see text) for the purpose of calculating an excited state redox potential value. ^d $E(3+/2+)$ values are vs. SCE values minus 0.03 V to give NHE values according to Lin et al.: *J. Am. Chem. Soc.* **1976**, *98*, 6536. $E(2+/1+)$ values are SCE values plus 0.07 V to give NHE values according to Creutz and Sutin: *Inorg. Chem.* **1976**, *13*, 496. Excited state potentials are calculated following these references. 1 eV = 8066 wavenumbers. ^e Lowering of bridging ligand π^* LUMO energy upon coordination of second Ru(bpy)₂²⁺ unit. This is the difference between the MLCT to BL absorption maxima *plus* the stabilization of the ruthenium(II) t_{2g} orbitals from the difference in $E(3+/2+)$ values, where applicable. ^f Reference 6 and this work. ^g Reference 7. ^h Reference 8. ^i Reference 9. ^j Reference 10. ^k Reference 11. ^l dpp = 2,3-bis(2-pyridyl)pyrazine. ppz = 4′,7′-phenanthrolino-5′,6′:5,6-pyrazine. BL(1) = 2,3-di-2-pyridylquinoxaline. BL(3) = 2,2′,3,3′-tetra-2-pyridyl-6,6′-biquinoxaline. BL(2) = 2,3,7,8-tetra-2-pyridylpyrazine-2,3-quinoxaline. bprym = 2,2′-bipyrimidine. dmbpyrm = 4,4′-dimethyl-2,2′-bipyrimidine. bbi = 2,2′-bibenzimidazole. biim = 2,2′-biimidazole.

rigid than bipyridine. The lifetime of $*Ru(bpy)_3{}^{2+}$ in fluid solution at room temperature is 600 ns, and the emission quantum yield is 0.38 at 77 K. The corresponding values for the tri-*o*-phenanthroline complex of Ru(II) are 900 ns and 0.60. In bimetallic complexes, the idea that flexibility may be important arises from a comparison of the 77 K emission spectra of the dpp and ppz complexes. Only the ppz complex shows a resolved vibrational progression of about 1200 cm^{-1}, indicating that a specific vibration dominates this transition. For the dpp complex, several ligand vibrations are equally effective in coupling the excited state to the ground state since no specific progression is resolved. The resonance Raman spectra of these complexes indicate specific modes which are strongly enhanced in resonance and are effective in coupling the ground to the excited state in absorption. Near the MLCT to ppz maximum, the spectrum is dominated by a mode at 1252 cm^{-1}. The corresponding dpp spectrum shows equally intense modes near 1250 and 1550 cm^{-1}. Taken together, these observations indicate that transitions between the ground and excited states are linked to a greater number of ligand vibrations for the more flexible dpp. In this case, they lead to more effective vibrational coupling to solvent and a greater rate of radiationless deactivation for the dpp complex.

The first oxidation potentials (Table III) for the ppz and dpp complexes fit a pattern observed for similar complexes with other bridging bis-diimine ligands. These serve to differentiate the pyrazine- and quinoxaline-based ligand systems (Table III, entries 1–5) from the others. For the pyrazine- and quinoxaline-based ligand complexes, the 3+/2+ oxidation potentials of the monometallic complexes are within experimental error the same as the first oxidation potentials of the bimetallic complexes (i.e., the 3+,2+/2+,2+ couple). Thus, for these bridging ligands, coordination of the second $Ru(bpy)_2{}^{2+}$ moiety does not affect the energy of the metal t_2 orbitals, and in the 2+,2+ state, little metal–metal interaction is evident. Consequently, the pronounced red shifts in the lower energy $t_2{\rightarrow}\pi*$ transitions to the bridging ligand originate in the decrease in energy of the $\pi*$ orbital. The calculated decrease in $\pi*$ acceptor orbital energies listed in Table III is within the range of such changes which occur when an electron-withdrawing substituent is present on the periphery of bipyridine in Ru(II) complexes. Thus, the second metal center in these bimetallic complexes acts as a mild electron withdrawing substituent. In Ru(II) complexes of this type where the substituent causes a large perturbation of the $\pi*$ acceptor orbital, the luminescent lifetime and emission intensity are either significantly reduced or not detectable.

Although the dpp and ppz dimer complex emissions appear rather unique for this class of complexes, on the basis of a more careful evaluation of the literature reports we propose that this may not, in fact, be the case. In a previous paper,[6] we suggested that the occurrence of emission from $[(bpy)_2Ru(dpp)Ru(bpy)_2]^{4+}$ might reflect a weakened interaction between metal centers, due to steric interactions of meta hydrogens on the pyridyl groups. However, since the bimetallic ppz complex emits at room temperature in solution, this clearly establishes that steric factors involving the bridging ligand are of minor importance in this context. In fact, the planar bridged ppz dimer shows a higher relative quantum yield for emission than the dpp dimer. This is surprising since the $\pi*$ acceptor orbital change for the ppz dimer is 3650 cm^{-1}, the largest among the ppz- and quinoxaline-based ligand complexes.

Rillema, Meyer, and co-workers[24] have pointed out that, within a series of analogous monometallic ruthenium(II) mixed-diimine complexes, the lowest MLCT transition energy correlates well with the first reduction potential of the complex, corresponding to the most easily reduced ligand. A similar correlation exists for the first five entries in Table III. More relevant to the emission properties of these complexes, however, is an approximate correlation (Figure 4) between the lowest energy MLCT band and the emission energy. This correlation suggests that the bimetallic
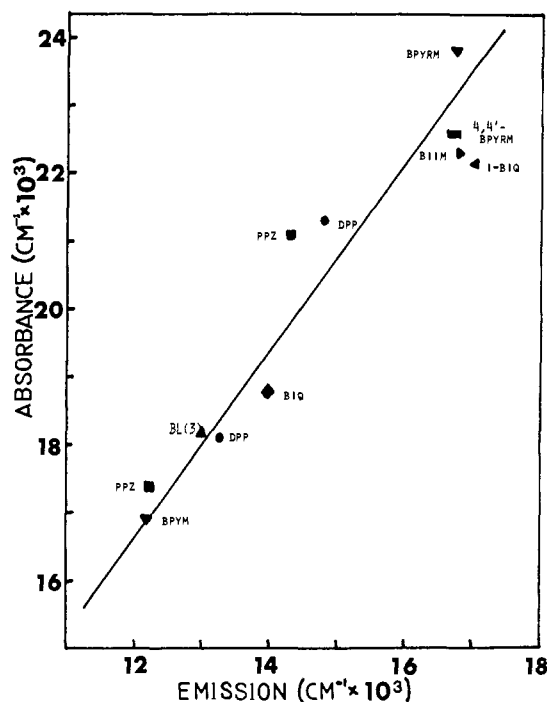
(24) Rillema, D. P.; Allen, G.; Meyer, T. J.; Conrad, D. *Inorg. Chem.* **1983**, *22*, 1617.

Figure 4. Correlation plot of emission energy vs. lowest energy MLCT (i.e., to bridging ligand) energy for complexes $(bpy)_2Ru(L)Ru(bpy)_2{}^{4+}$ (L = bisdiimine). See Table III for L codes. Also, biq = 2,2'-biquinoline and i-biq = 2,2'-biisoquinoline.

complexes utilizing the bridging ligands which are quinoxaline based would exhibit emission maxima beyond 850 nm. Since this would place the maxima beyond the detection limit of typical emission systems in use at the time of these reports, absence of reported emission is probably not indicative that these complexes do not emit. This is not to imply that the interaction between metal centers is not important since this interaction leads to the decrease in energy of the $\pi*$ acceptor orbital for the dimer relative to the monomer. Since this shifts the emission beyond 850 nm, the larger interaction between metal centers is an important factor in producing complexes for study.

It is not immediately apparent if a similar explanation applies for the bimetallic bipyrimidine or biimidazole complexes. In $[(bpy)_2Ru(bpyrm)Ru(bpy)_2]^{4+}$, the lower energy MLCT transition to the bpyrm occurs at 592 nm. The absorption maximum is within the range of those for the quinoxaline-based ligand complexes, and by analogy the emission may occur beyond the detection limits for solutions. It is notable that maxima were reported for the solid at 769 and 870 nm. For the 4,4'-dimethylbipyrimidine dimer, however, the lower energy MLCT band occurs at 578 nm, comparable to the ppz bimetallic complex. In the absence of strong metal–metal interaction, a similar emission energy is expected. The bpym and biim complexes differ from the others in Table III with regard to this criterion. The first oxidation potentials of the mono- and bimetallic complexes differ by about +0.18 and −0.37 V, respectively. As previously noted, this indicates a ground-state metal–metal interaction in which the metal-centered t_2 orbitals are raised and lowered, respectively. The interactions between the metal centers in the excited states are more pronounced as indicated by the lowering of the $\pi*$ acceptor orbital energies. These data do not establish whether the bpym and biim complexes are expected to be luminescent, but they suggest that, since the metal centers are strongly coupled, the emission, if present, will be red shifted and the intensity likely will be very low. Neither situation is appealing with respect to excited state redox chemistry.

The excited state redox potentials of the mono- and bimetallic complexes are listed in Table III. For the ppz and dpp complexes, the calculation is based on the measured emission maximum. Since the actual 0–0 transitions will lie to higher energy in each case, these potentials are in fact underestimated. The calculated

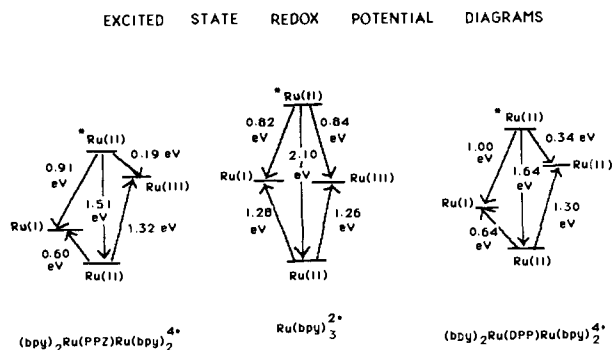EXCITED   STATE   REDOX   POTENTIAL   DIAGRAMS

Figure 5. Excited-state potential diagrams comparing Ru(bpy)$_3^{2+}$ (center) to dimeric complexes of dpp (right) and ppz (left). See Table III for reference potentials.

potentials of the bimetallic complexes for the quinoxaline-based ligand complexes (entries 3 to 5) are estimated from the correlation in Figure 4. In spite of these approximations, the excited state potentials listed in Table III clearly indicate that MLCT states of these kinds of binuclear complexes are invariably weaker reductants than their monometallic counterparts. The decrease in MLCT state 2+*/3+ potential arises principally in the decline in energy in the π^* acceptor orbital, since ground-since oxidation potentials of the mono- and bimetallic analogues are the same within experimental error. In contrast, the MLCT states of the bimetallic complexes are stronger oxidants than their corresponding monometallic analogues since the decrease in the energy of the π^* acceptor orbital is more than offset by a decrease in the ground-state reduction potential (i.e., for the bridging ligand). In fact, as illustrated in Figure 5, the bimetallic dpp and ppz complexes are stronger excited-state oxidants than *Ru(bpy)$_3^{2+}$. Also of note, in view of the recognized difficulties in controlling the reversibility of the photoredox chemistry of Ru(bpy)$_3^{2+}$, is the significant reduction in the ground-state reduction potentials, which lowers the driving force for the thermal back reaction. With the appropriate choice of a weak reducing quencher, reductive quenching of these bimetallic complexes can be used to transfer an electron to a second oxidant by means of a second thermal reaction. Although the fraction of radiant energy converted to redox potential is small, the overall reaction, i.e., oxidation of a quencher and reduction of the second oxidant, will not be burdened by an exergonic back reaction. Quenching experiments are in progress to test the calculated MLCT state potentials and the possibility of utilizing the above scheme to reduce viologens or other desirable electron-transfer intermediaries.

Conclusions

The detection of emission from binuclear complexes of Ru(II) of the type [(bpy)$_2$Ru-L-Ru(bpy)$_2$]$^{4+}$ at room temperature in fluid solution is closely correlated with the energy of the bridging ligand π^* acceptor orbital, which, along with the ground-state oxidation and reduction potentials, is a monitor of the degree of interaction between the two Ru(bpy)$_2^{2+}$ units as moderated by the bridging ligand. The excited-state redox potentials of binuclear complexes with dpp and ppz are luminescent, and their MLCT states are calculated to be weak reductants but surprisingly potent oxidants.

Unsymmetrically, Chemically Activated 1,2-Dicyclopropylacetylene: An Example of Restricted Energy Flow?

W. von E. Doering*[†] and William J. Ehlhardt

Contribution from the Department of Chemistry, Harvard University, Cambridge, Massachusetts 02138-2902. Received November 19, 1986

Abstract: The Doering–Gilbert–Leermakers strategy for revealing chemical reaction possibly more rapid than internal flow of energy is applied to 1,2-dicyclopropylacetylene by examining addition of dideuteriomethylene to 1-cyclopropyl-2-vinylacetylene and of methylene to 1-(2,2-dideuteriocyclopropyl)-2-vinylacetylene in the gas phase. This reduction to practice of the general strategy has three advantages: one of the three isomers of allylcyclopropylacetylene, itself the key product of chemically activated rearrangement, bears internal witness to the achievement of structural symmetry prior to its generation; the long, linear acetylenic linkage precludes internal energy flow by a mechanism of intramolecular collision; and the activation energy of the cyclopropane–propene rearrangement is lowered significantly. Analysis of the experimental results reveals a small amount of rearrangement at high pressures occurring prior to complete symmetrization of structure and/or energy. If this observation can be ascribed to incomplete symmetrization of *energy*, the basic premise of the Rice–Ramsperger–Kassel–Marcus theory—that internal energy flow be so much faster than chemical reaction that a structureless statistical treatment is justified—may require reconsideration.

Rice–Ramsperger–Kassel–Marcus (RRKM) theory of unimolecular, gas-phase processes supposes an internal flow of energy so much faster than chemical reaction that a structure-free, statistical theory is applicable.[1] Efforts to define the experimental

limits of this premise begin with the work of Kistiakowsky and Butler[2] and continue into the present era of multiphoton infrared

(1) For references to earlier reviews and recent work, see: Holbrook, K. A. *Chem. Soc. Rev.* **1983**, *12*, 163–211. Goodall, D. M.; Cureton, C. G. *Chem. Brit.* **1983**, 493–501.
(2) Butler, J. N.; Kistiakowsky, G. B. *J. Am. Chem. Soc.* **1960**, *82*, 759–765.